*diversity*

MDPI

*Article*

# *Anianabacter salinae* gen. nov., sp. nov. ASV31$^T$, a Facultative Alkaliphilic and Extremely Halotolerant Bacterium Isolated from Brine of a Millennial Continental Saltern

**Maia Azpiazu-Muniozguren [1], Minerva García [1], Lorena Laorden [1,2], Irati Martinez-Malaxetxebarria [1,2], Sergio Seoane [3], Joseba Bikandi [1], Javier Garaizar [1,2] and Ilargi Martínez-Ballesteros [1,2,*]**

[1] MikroIker Research Group, Department of Immunology, Microbiology and Parasitology, Faculty of Pharmacy, University of the Basque Country UPV/EHU, Paseo de la Universidad 7, 01006 Vitoria-Gasteiz, Álava, Spain
[2] Bioaraba, Microbiology, Infectious Disease, Antimicrobial Agents and Gene Therapy, 01006 Vitoria-Gasteiz, Álava, Spain
[3] Plant Biology and Ecology Department, Faculty of Science and Technology, University of the Basque Country UPV/EHU, Barrio Sarriena s/n, 48940 Leioa, Bizkaia, Spain
* Correspondence: ilargi.martinez@ehu.eus

**Abstract:** During a prokaryotic diversity study in Añana Salt Valley, a new *Rhodobacteraceae* member, designated ASV31$^T$, was isolated from Santa Engracia spring water. It was extremely halotolerant, tolerating up to 23% NaCl, and facultatively alkaliphilic, growing at pH 6.5–9.5 (optimum at 7.0–9.5). The isolate was a Gram-negative, rod-shaped, aerobic and non-motile bacterium that formed beige-to-pink colonies on marine agar. According to a 16S rRNA gene-based phylogenetic analysis, strain ASV31$^T$ forms a distinct branch of the family *Rhodobacteraceae*, with *Thioclava pacifica* DSM 10166$^T$ being its closest type strain (95.3%). This was confirmed with a phylogenomic tree and the values of ANI (73.9%), dDDH (19.3%), AAI (63.5%) and POCP (56.0%), which were below the genus/species level boundary. Additionally, an ability to degrade aromatic compounds and biosynthesise secondary metabolites was suggested by the genome of strain ASV31$^T$. Distinguishing fatty acid profiles and polar lipid content were also observed. The genome size was 3.6 Mbp, with a DNA G+C content of 65.7%. Based on the data obtained, it was considered that strain ASV31$^T$ (=CECT 30309$^T$ = LMG 32242$^T$) represents a new species of a new genus in the family *Rhodobacteraceae*, for which the name *Anianabacter salinae* gen. nov., sp. nov. is proposed.

**Keywords:** continental saltern; extremely halotolerant bacteria; alkaliphilic; *Anianabacter salinae*; biotechnological applications



**Citation:** Azpiazu-Muniozguren, M.; García, M.; Laorden, L.; Martinez-Malaxetxebarria, I.; Seoane, S.; Bikandi, J.; Garaizar, J.; Martínez-Ballesteros, I. *Anianabacter salinae* gen. nov., sp. nov. ASV31$^T$, a Facultative Alkaliphilic and Extremely Halotolerant Bacterium Isolated from Brine of a Millennial Continental Saltern. *Diversity* **2022**, *14*, 1009. https://doi.org/10.3390/d14111009

Academic Editors: Michael Wink and Stuart Donachie

Received: 25 September 2022
Accepted: 18 November 2022
Published: 21 November 2022



## 1. Introduction

Solar salterns are extreme habitats in which halophilic microorganisms with different adaptations to such environments are found. For this reason, the study of microbial communities of these environments is important, not only to increase knowledge around their diversity, but also because the metabolites produced by members of these communities could be interesting for different biotechnological applications. An active continental solar saltern, located in Añana Salt Valley (Álava, Northern Spain, 42.82 N 2.98 W), was recently declared a Globally Important Agricultural Heritage System by the Food and Agriculture Organization of the United Nations (FAO). Its origin lies in the marine water of the Triassic period (between 251 and 208 million years ago), when a diapir was formed by the deposit of evaporite layers that rose through the Earth's surface, resulting in the hypersalinity of the water that is now found in this valley [1]. During a study of the microbial diversity of this saltern, a beige- to pink-pigmented bacterial strain from the Santa Engracia spring (the main brine support for the salt production in the saltern) was isolated. The isolate was designated ASV31$^T$, which represented a potential novel species of a novel genus in the *Rhodobacteraceae* family.

The family *Rhodobacteraceae*, belonging to the order *Rhodobacterales*, class *Alphaproteobacteria*, was first proposed in 2005 by Garrity et al. [2] and was amended by Hördt et al. in 2020 [3]. This family is a large phenotypically, metabolically and ecologically diverse taxonomic group. Most members of the family originated from aquatic environments and many of them require sodium ions or combined salts for growth [4]. At the time of writing, the family *Rhodobacteraceae* consists of 227 validly published genera, including synonyms (https://lpsn.dsmz.de/family/rhodobacteraceae, accessed on 20 January 2022) which are divided into six different phylogenetic subgroups: *Stappia*, *Amaricoccus*, *Paracoccus*, *Rhodobacter*, *Rhodovulum* and *Roseobacter* [5]. The latter has been proposed to be split from the *Rhodobacteraceae* family to form a new one, the *Roseobacteraceae* family [6]. In general, members of the family *Rhodobacteraceae* are Gram-negative and multiply by binary fission or budding, following monopolar growth. While they are mainly aerobic photo- and chemoheterotrophs, purple non-sulphur bacteria that perform photosynthesis in anaerobic environments are also found. They are characterised chemotaxonomically by the presence of ubiquinone-10 (Q-10) and C18:1 ω7c is the predominant cellular fatty acid. They are considered to be the major group of marine heterotrophic bacteria and have different roles such as contributing to sulphur, nitrogen and carbon cycles, decomposing various compounds and generating secondary metabolites [7,8].

Members of the *Rhodobacteraceae* family could be utilised for industrial applications. Exopolysaccharide (EPS)-producing species, such as *Palleronia marisminoris* [7], can be found in this family. Microbial EPSs can be used in the food industry as viscosity agents, stabilisers, emulsifiers, gelling agents and water-binding agents. Moreover, in the medical industry, microbial EPSs are emerging as promising materials for drug-release systems, due to their ability to retain large amounts of water and remain insoluble, as well as drug-targeting carriers, based on their particular binding and penetrating features to cellular receptors [9]. Other genera, such as *Methylarcula,* are able to synthesise ectoine as a major compatible solute [5]. Ectoine is commercially available as a protectant of proteins, DNA and mammalian cells [10]. Others, such as *Palleronia*, *Salipiger* and *Tranquillimonas*, can synthesise polyhydroxyalkanoates (PHAs), or, more commonly, polyhydroxybutyrate (PHB), as a carbon reserve material [5]. PHAs are a family of biodegradable and biocompatible polyesters accumulated by many microorganisms and are developed for industrial usage (e.g., as bioplastics, biofuels and fine chemicals) or for medicinal use [10]. Furthermore, extremophilic carbohydrate-active enzymes (CAZymes) have recently garnered a lot of attention due to their advantages [11]. In this context, a genomic annotation allows for the identification of various metabolic pathways either directly involved or not in the synthesis of these metabolites of industrial interest.

Using a polyphasic approach, the aim of this study was to characterise the strain ASV31$^T$ (isolated from the brine of a saltern) and to determine its taxonomic position within the family *Rhodobacteraceae*.

## 2. Materials and Methods

### *2.1. Strain Isolation and Maintenance*

Strain ASV31$^T$ was isolated from the Santa Engracia natural spring in the continental saltern at Añana Salt Valley, located 598 m above sea level (the approximate geographic coordinates are 42.79 N 2.98 W). Water samples were collected in June 2016. The water temperature was 16.0 °C, pH 6.6 and salt content 20%. In order to isolate halophilic and halotolerant bacteria, the water samples were first processed through multiple filtration steps (Whatman® Grade 113 V, Maidstone, UK, and Millipore 5 µm and 0.22 µm filters (Burlington, MA, USA)). Subsequently, 100 µL of filtered water was cultivated on marine agar (MA; Conda) and incubated at 25 °C. After 7 days of incubation, a visible beige-to-pink colony was observed and subcultured on MA, until pure culture was obtained. Strain ASV31$^T$ was stored at −80 °C in marine broth (MB; Conda) and 25% (*v*/*v*) glycerol.

### 2.2. 16S rRNA Gene-Based Identification and Phylogeny

Strain ASV31$^T$ chromosomal DNA was extracted from three-day colonies on MA using PrepMan Ultra Reactive (Applied Biosystems, Waltham, MA, USA) following the manufacturer's specifications. The DNA concentration was measured using a NanoDrop 2000 spectrophotometer (Thermo Scientific, Waltham, MA, USA). 16S rRNA gene sequencing was used for strain identification. The gene was amplified using the universal bacterial primers 27F (5′-AGAGTTTGATCMTGGCTCAG-3′) and 1492R (5′-GGTTACCTTGTTACGACTT-3′) [12], and was, subsequently, purified by a NucleoSpin Gel and PCR clean-up kit (Macherey-Nagel, Düren, Germany). Purified PCR products were sequenced using the Sanger method (Stab Vida, Caparica, Portugal) and the sequencing data were analysed with Chromas 2.6.6 software (Technelysium, South Brisbane, Australia). Identification of closely related species and the measurement of their 16S rRNA sequence similarity were carried out using the EzBioCloud database (www.ezbiocloud.net/identify, accessed on 15 June 2021) [13].

The 16S rRNA gene sequences of representatives of the family *Rhodobacteraceae* were retrieved from the GenBank database and a phylogenetic tree was constructed with MEGA X software [14] using the neighbour-joining [15], minimum-evolution [16] and maximum-likelihood [17] methods. Evolutionary distance matrices were calculated using the algorithm of Kimura's two-parameter model with bootstrap values based on 1000 replications [17].

### 2.3. Phenotype and Chemotaxonomy

Type strains *Thioclava pacifica* DSM 10166$^T$ and *Rhodovulum algae* LMG 29228$^T$ were tested alongside ASV31$^T$ for comparison. The phenotypic characteristics of cells and colonies were determined after three days of growth at 30 °C on MA. Cell morphology, size and presence of flagella were determined with transmission electron microscopy (1400 Plus, JEOL, Tokyo, Japan) at the UPV/EHU Advanced Research Facilities (SGIker, Leioa, Spain). Gram staining was performed using the method described by Smith et al. [18]. Cellular pigments were analysed by HPLC. Pigment extraction was performed with 90% acetone following the method described by Zapata et al. [19], with the modifications explained by Seoane et al. [20]. The absorbance chromatogram was extracted at 440 nm. PHA production was tested using Sudan black B staining according to the procedures of Smith et al. [21] and Santhanam et al. [22], inoculating 10 mL of MB supplemented with glucose (2% $w/v$) and yeast extract (2 g/L) as the carbon and nitrogen sources, respectively, and incubating this for 48 h at 28 °C and 150 rpm. Cell motility was measured using the hanging drop method in semisolid agar including MB and 0.7% bacteriological agar (Condalab, Madrid, Spain). Anaerobic growth was tested at 30 °C for 15 days on MA in an anaerobic chamber with GENbox anaer (bioMérieux, Marcy-l'Étoile, France). Growth at different temperatures (4, 8, 15, 20, 25, 30, 37 and 42 °C) was determined on MA after 3 to 15 days of incubation. Salt tolerance and requirement for growth were tested in MB supplemented with NaCl at final concentrations of 0, 0.5, 1.0, 2.0, 3.0, 5.0, 10.0, 15.0, 20.0 and 23.0 g/L. These media were prepared according to the MB formula, but without NaCl. The pH range supporting growth was determined in MB at 30 °C, with the pH adjusted (pH 4.5–10.5 in increments of 0.5 pH units) with different buffers: sodium acetate/acetic acid (for pH 4.5–6.0) and $NaHCO_3/Na_2CO_3$ (for pH 6.5–10.5). Energetic metabolism was characterised on a modified MA medium for photo- (anaerobic, light 2400 lx) and chemo- (aerobic, dark)organoheterotrophy (with pyruvate (0.03%, $w/v$) as the carbon source/electron donor), photolithoautotrophy (anaerobic, light (2400 lx), with $Na_2S_2O_3.5H_2O$ (1 mM) as the electron donor and $NaHCO_3$ (0.1%, $w/v$) as the carbon source), chemolithoautotrophy (dark, aerobic, with $Na_2S_2O_3.5H_2O$ (1 mM) as the electron donor and $NaHCO_3$ (0.1%, $w/v$) as the carbon source) and fermentative growth (dark, anaerobic, with pyruvate/glucose (0.3%, $w/v$) as the fermentable substrates).

Oxidase activity was tested with Bactident Oxidase strips (Merck, Rahway, NJ, USA) and catalase activity with ID colour catalase (bioMérieux). Hydrolysis capacity was determined on MA plates supplemented with 1% ($w/v$) skimmed milk, 1% ($w/v$) Tween 20 and

1% (*w*/*v*) Tween 80. Other physiological and biochemical features were examined using API ZYM and API 20NE strips (bioMérieux) according to the manufacturer's instructions, with cells suspended in a saline solution. Susceptibility to antibiotics was tested on MA plates incubated at 30 °C for three days using discs containing the following: ciprofloxacin (10 µg), erythromycin (15 µg), ofloxacin (5 µg), penicillin G (5 IU), cephazolin (30 µg), rifampicin (2 µg), kanamycin (5 µg), gentamicin (10 µg), polymyxin B (300 IU), vancomycin (30 µg) and streptomycin (10 µg).

Whole-cell fatty acid composition was determined following the protocol recommended by the MIDI Microbial Identification System [23] at the Spanish Type Culture Collection (CECT). Identification was performed with the Sherlock MIDI version 6.1 and cellular fatty acid content was analysed using the TSBA6 library [24]. Cells were grown for 72 h at 30 °C on MA to obtain their biomass. Analyses of polar lipids and respiratory quinones were carried out using the Identification Service at the Leibniz-Institut DSMZ (Deutsche Sammlung von Mikroorganismen und Zellkulturen GmbH, Braunschweig, Germany) following the protocol based on Bligh and Dyer [25] and Tindall et al. [26].

### *2.4. Genome Sequencing and Analysis*

Whole-genome sequencing of the ASV31$^T$ isolate was performed using the Illumina Miseq platform at the UPV/EHU Advanced Research Facilities (SGIker). DNA extraction was conducted using the NucleoSpin Tissue DNA extraction kit (Macherey-Nagel) according to the manufacturer's protocol. Assembly from raw paired-end reads to contigs was performed using the SPAdes assembler v3.13.0 available in PATRIC 3.6.9 software [27]. Authenticity was confirmed with the presence of the 16S rRNA gene sequence obtained using PCR on the assembled genome, and the genome's quality was confirmed using CheckM v1.0.18 [28].

Genome-based comparisons of strain ASV31$^T$ with its closest species were performed with average nucleotide identity (ANI) values computed using the OrthoANI Calculator tool available at EzBiocloud (www.ezbiocloud.net/tools/ani, accessed on 20 January 2022) [29] and digital DNA–DNA hybridisation (dDDH) values computed using the genome-to-genome distance calculator (http://ggdc.dsmz.de/ggdc.php, accessed on 20 January 2022) [30]. In order to assess genus affiliations, amino acid-level comparisons were performed using the average amino acid identity (AAI) and percentage of conserved proteins (POCP) for every pairwise combination of genomes. The AAI values were calculated using the Kostas Lab AAI calculator (http://enve-omics.ce.gatech.edu/aai/, accessed on 20 January 2022) [31]. The POCP values were calculated using a Python script with the formula $[(C1 + C2)/(T1 + T2)] \times 100\%$, where C1 and C2 represent the conserved number of proteins in the two genomes being compared, and T1 and T2 represent the total number of proteins in the two genomes being compared [32].

A whole-genome-based taxonomic analysis was performed on the Type Strain Genome Server (https://tygs.dsmz.de, accessed on 18 February 2022) [30] and a genome-based phylogenetic tree was inferred with FastME 2.1.6.1 [33] from the GBDP distances calculated from genome sequences. Branch lengths were scaled in terms of GBDP distance formula d5. In order to provide further information about the taxonomic position of strain ASV31$^T$, the amino acid sequences of RpoC, 2-oxoglutarate dehydrogenase and acyl-CoA synthetase proteins were obtained from the genome. These sequences were analysed with BLAST in order to find the most similar taxa. Phylogenetic trees based on these proteins were constructed with MEGA X using the maximum-likelihood method. Amino acid sequences were retrieved from the GenBank database.

Gene annotation was performed using the NCBI Prokaryotic Genome Annotation Pipeline and the Rapid Annotation with Subsystems Technology (RAST) pipeline [34]. The detection of gene clusters related to secondary metabolite production was performed using the antiSMASH 6.0.1 webserver (https://antismash.secondarymetabolites.org, accessed on 11 May 2022) [35]. The dbCAN meta server (https://bcb.unl.edu/dbCAN2/, accessed on

25 May 2022) [36] was used to identify the coding sequences (CDSs) encoding carbohydrate-active enzymes (CAZymes) using an HMMER annotation.

## 3. Results and Discussion

A polyphasic study was carried out in order to characterise strain ASV31$^T$, which was isolated from a hypersaline water spring in an active continental saltern. This saltern was formed as a result of the deposit of evaporites millions of years ago during the desiccation of the great ocean that covered almost the entire Earth.

### *3.1. 16S rRNA Gene-Based Identification and Phylogeny*

Phylogenetic analysis showed that strain ASV31$^T$ belonged to the Bacteria domain, *Proteobacteria* phylum, *Alphaproteobacteria* class, *Rhodobacterales* order and *Rhodobacteraceae* family. Due to the short 16S rRNA gene sequence (1337 bp) obtained by PCR (sequence deposited at GenBank under accession number MW691205), the 1468 bp 16S rRNA sequence from genome sequencing was used for further phylogenetic analysis (accession number JAHQZS010000014.1). A comparison of 16S rRNA sequences determined that *Thioclava* GU322906_s YC6923 was the most closely related strain (95.4% similarity between sequences), followed by *Thioclava pacifica* DSM 10166$^T$ (95.3%) and *Thioclava sediminum* TAW-CT134$^T$ (95.2%) type strains. Other related taxa were *Tropicimonas* AM176881_s SZB22 (95.1%), *Haematobacter massiliensis* CCUG 47968$^T$ (95%) and *Rhodovulum adriaticum* DSM 2781$^T$ (94.9%). Hördt et al. [3] proposed that when the 16S rRNA gene sequence similarity is below 95%, the taxa represent different genera. The similarity of the 16S rRNA sequences of *Thioclava* species and strain ASV31$^T$ was just at this limit, which was not sufficient to support the placement of strain ASV31$^T$ into the *Thioclava* genus. Furthermore, the phylogenetic tree, constructed with the neighbour-joining method based on the 16S rRNA gene sequence, showed that strain ASV31$^T$ was not defined by any genus in the family *Rhodobacteraceae*, as it clustered in a differentiated branch between the *Rhodobacter* and *Roseobacter* groups (Figure 1). In fact, strain ASV31$^T$ was in an independent branch that did not show a defined affiliation either to *Thioclava* spp. (*Rhodobacter* group) or *Tropicimonas* spp. (*Roseobacter* group). Similar results were observed in both the maximum-likelihood and the minimum-evolution trees (Figures S1 and S2). These results suggested that strain ASV31$^T$ may represent a novel genus of the *Rhodobacteraceae* family.

### *3.2. Phenotypic and Chemotaxonomic Characterisation*

Strain ASV31$^T$ is a Gram-negative bacillus 2.4–2.5 µm in length and 0.4–0.5 µm in width, with a mucous polysaccharide capsule (slime) all around (Figure 2A). This feature was also seen genetically in the metabolic reconstruction (results shown below). Unlike *Thioclava* members, which are described as rarely motile by means of a polar flagellum [37], and *Rhodovulum* members, which also exhibit motility by a polar flagellum [5], no flagella were observed in ASV31$^T$ using transmission electron microscopy. Motility was neither observed using the hanging drop method nor in semisolid agar. The presence of PHA as intracellular granules was confirmed through Sudan black B staining (Figure 2B). This capacity has also been reported in *Rhodobacter capsulatus*, *Palleronia marisminoris*, *Salipiger* spp., *Tranquillimonas* spp., *Labrenzia* spp. and *Rhodovulum sulfidophilum* in the *Rhodobacteraceae* family, with PHB being the main PHA class [5].

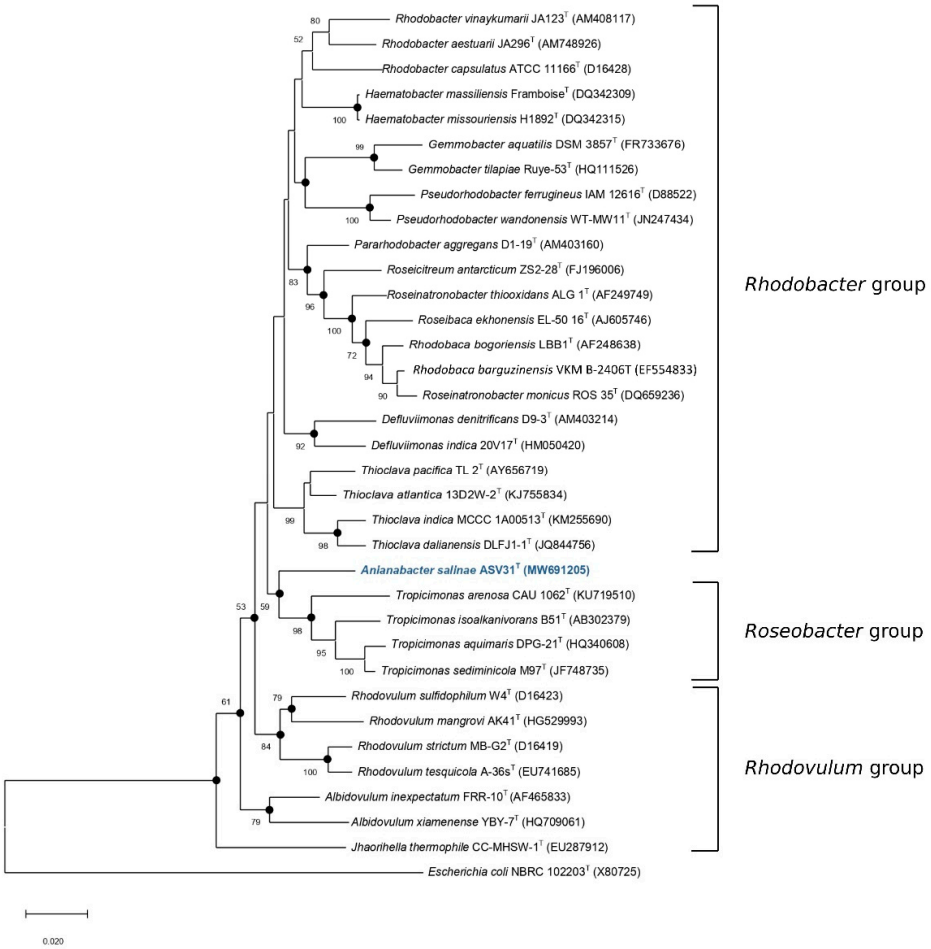


**Figure 1.** Neighbour-joining phylogenetic tree based on 16S rRNA gene sequences that shows the relationship between strain ASV31$^T$ and the type strains of *Rhodobacter*, *Roseobacter* and *Rhodovulum* groups of the family *Rhodobacteraceae*. The black circles indicate the clades that were also conserved in both the maximum-likelihood and minimum-evolutionary phylogenetic trees. Bootstrap values (expressed as percentages of 1000 replications) greater than 50% in the clade nodes are shown. *Escherichia coli* NCCB 54008$^T$ was used as outgroup. Scale: 0.02 substitutions per nucleotide position.

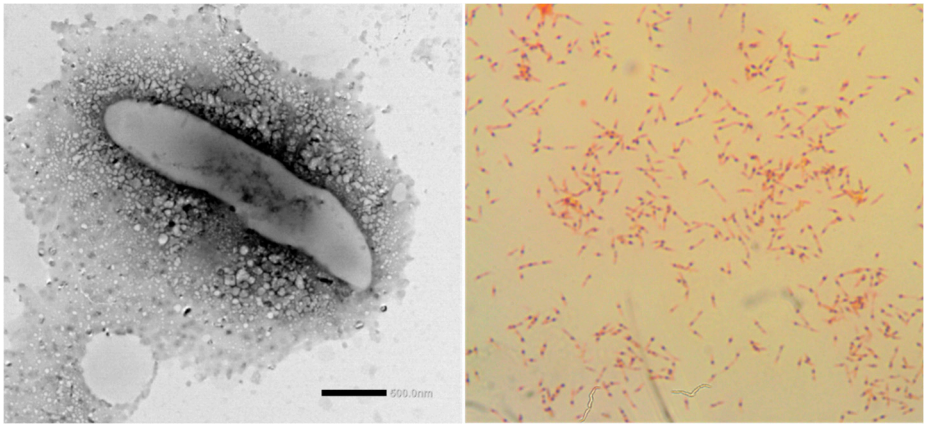


(**a**) (**b**)

**Figure 2.** *Anianabacter salinae* ASV31$^T$ cell characteristics observed using microscopy: (**a**) Transmission electron micrograph of a cell. A polysaccharide mucous capsule was observed around the cell and darker spots in the cytoplasm. Bar 500.0 nm. (**b**) Sudan black B staining of PHA granules observed as black intracellular granules under 100× oil immersion objective.

Colonies of strain ASV31$^T$ were less than 1 mm in diameter and beige-to-pink coloured, with a circular shape, convex elevation, transparent smooth edge and they glistened on the MA medium (Figure S3). The colony morphology was different from the *Thioclava pacifica* DSM 10166$^T$ and *Rhodovulum algae* LMG 29228$^T$ strains that were studied alongside ASV31$^T$ in this study. ASV31$^T$ was not capable of growing under anaerobic conditions. Strain ASV31$^T$ grew in a temperature range of 18–37 °C, with an optimum temperature of 30 °C, the same as its relatives. The pH range for growth was pH 6.5–9.5, with an optimum of pH 7.0–9.5, indicating it was slightly alcaliphilic compared with its close relatives. The NaCl tolerance for growth was 0.0–23.0%, with an optimum of 3.0–5.0%. In contrast with its relatives, strain ASV31$^T$ could grow at higher salt concentrations and did not require NaCl to grow like most *Thioclava* and *Rhodovulum* members [5]. Members of *Rhodobacteraceae* are mainly aerobic photo- and chemoheterotrophs [5]. In this sense, strain ASV31$^T$ is an aerobic chemoorganoheterotroph. This capacity was also observed in *Thioclava pacifica* DSM 10166$^T$ and *Rhodovulum algae* LMG 29228$^T$. Chemolitoautotrophic, photolithoautotrophic and photoorganoheterotrophic growth could not be demonstrated in ASV31$^T$. Moreover, *Thioclava* members are considered facultative sulphur chemolithotrophs, are included in the *Rhodobacter* group and are able to grow using thiosulfate oxidation and inorganic carbon fixation through the Calvin cycle [5]. This characteristic was observed in this study. Photorganoheterotrophy was also observed in *Rhodovulum algae* LMG 29228$^T$ (as described by Ramaprasad et al. [38]). Fermentative growth was not seen in any of the strains analysed, as described in [5].

Spheroidenone was the main pigment in ASV31$^T$, while spheroidene and bacteriochlorophyll a (BChl a) were also detected in the strain. It is known that *Rhodovulum* members can also synthesise BChl a and carotenoids of the spheroidene series (spheroidene, spheroidenone, demethylspheroidene, hydroxyspheroidene and neurosporene, among others) in different proportions. However, *Thioclava* members do not synthetise BChl a or carotenoids [5,39].

Oxidase activity was positive in ASV31$^T$ and its relatives, while catalase was present in ASV31$^T$ and *Rhodovulum algae* LMG 29228$^T$. Urease was only present in *Rhodovulum algae* LMG 29228$^T$. A capacity for Tween 20 hydrolysis was only seen in strain ASV31$^T$ and none of the strains had a casein or Tween 80 hydrolysis ability. In API 20NE tests, ASV31$^T$ was positive for aesculin hydrolysis and nitrate reduction, but negative for indole production, glucose fermentation, gelatine hydrolysis, arginine dihydrolase, urease and β-galactosidase, and the assimilation of glucose, arabinose, mannose, mannitol, N-acetylglucosamine, maltose, gluconate, caprate, adipate, malate, citrate and phenylacetate. The API ZYM tests showed alkaline phosphatase, esterase (C 4), esterase lipase (C 8), leucine arylamidase, valine arylamidase and α-glucosidase activity, weak activity of cysteine arylamidase, acid phosphatase and naphthol-AS-BI- phosphohydrolase, and negative activity of lipase (C 14), α-chymotrypsin, trypsin, α- and β-galactosidases, β-glucuronidase, β-glucosidase, N-acetyl-β-glucosaminidase, α-mannosidase and α-fucosidase. Strain ASV31$^T$ was resistant to polymyxin B (300 IU), vancomycin (30 μg) and streptomycin (10 μg). The most relevant phenotypic characteristics that distinguished strain ASV31$^T$ from its closest relatives are summarised in Table 1.

**Table 1.** Major phenotypic characteristics that distinguished ASV31$^T$ from its closest relatives. Strains: 1, ASV31$^T$ (this study); 2, *Thioclava pacifica* DSM 10166$^T$ (this study); 3, *Rhodovulum algae* LMG 29228$^T$ (this study); 4, *Tropicimonas isoalkanivorans* B51$^T$ [40]; 5, *Haematobacter massiliensis* CCUG 47968$^T$ [41]. +, positive; −, negative; w, weakly positive; NA, no data available; ND, not determined. All the strains were positive for oxidase. In API ZYM strips, all the strains were positive for alkaline phosphatase, leucine arylamidase and negative for lipase (C 14), trypsin, α-chymotrypsin, α-galactosidase, β-galactosidase, β-glucuronidase, N-acetyl-β-glucosaminidase, α-mannosidase and α-fucosidase.

| Characteristics | 1 | 2 | 3 | 4 | 5 |
|---|---|---|---|---|---|
| Cell shape | Rod | Rod | Rod | Rod | Rod |
| Gram staining | - | - | - | - | - |
| Motility | - | + | + | + | - |
| Colony colour | Beige to pink | Beige | Maroon | White | Not pigmented |
| Growth range (optimum): | | | | | |
| NaCl (% *m/v*) | 0–23 (3–5) | 1–10 (3–5) | 0–10 (2–5) | 1–6 | NA |
| Temperature (°C) | 18–37 (30) | 8–42 (30) | 4–42 (30) | 10–46 (37) | NA |
| pH | 6.5–9.5 (7–9.5) | 6.0–9.5 (6.0) | 6.0–9.5 (6.0) | 5.5–8.0 | NA |
| Anaerobic growth | - | - | + | - | - |
| Photoorganoheterotrophy | - | - | + | NA | NA |
| Chemolithoautotrophy | - | + | ND | - | NA |
| Photolithoautotrophy | - | - | - | NA | NA |
| Catalase test | + | - | + | - | + |
| Urease test | - | - | + | NA | + |
| Hydrolysis of: | | | | | |
| Casein | - | - | - | NA | NA |
| Tween 20 | + | - | - | - | NA |
| Tween 80 | - | - | - | - | NA |
| Aesculin | + | + | + | NA | - |
| Assimilation of: | | | | | |
| Malate | - | - | w | NA | NA |
| Enzymatic activities: | | | | | |
| Esterase (C 4) | + | w | w | NA | + |
| Esterase lipase (C 8) | + | w | - | NA | + |
| Valine arylamidase | + | - | w | NA | - |
| Acid phosphatase | w | w | + | NA | + |
| Naphthol-AS-BI-phosphohydrolase | w | w | + | NA | w |
| Cystine arylamidase | w | - | - | NA | - |
| α-glucosidase | + | + | - | NA | - |
| β-glucosidase | - | w | - | NA | - |
| Pigments | Spheroidenone, spheroidene and BChl a | Not detected [1,a] | Spheroidenone and BChl a [1,a,b] | ND | ND |

[1] Data from: a, Sorokin et al. [39]; b, Ramaprasad et al. [38].

The major fatty acids detected in strain ASV31$^T$ were C19:0 cyclo ω8c (38.16%) and Summed Feature 8 (37.34%) (Table 2). Notably, the main fatty acid, C19:0 cyclo ω8c, in strain ASV31$^T$ was not present in *Thioclava pacifica* DSM 10166$^T$ or *Rhodovulum algae* LMG 29228$^T$. Moreover, Summed Feature 8 was the major fatty acid found in *Thioclava pacifica* DSM 10166$^T$ (83.08%) and *Rhodovulum algae* LMG 29228$^T$ (70.12%), while in ASV31$^T$ it was detected at a lower percentage (37.34%). Moreover, ASV31$^T$ was the only strain that had no hydroxy fatty acids in its composition and was the only strain with unsaturated fatty acids.

The polar lipid profile of strain ASV31$^T$ comprised phosphatidylglycerol, aminolipid, two unidentified glycolipids, two unidentified phospholipids and two unidentified lipids (Figure S4). It was observed that phosphatidylethanolamine and phosphatidylglycerol, which are among the major polar lipids in *Thioclava dalianensis* and *Rhodovulum* members [5,37], did not match with the profile of strain ASV31$^T$. Ubiquinone Q-10 was detected in strain ASV31$^T$, which is characteristic of most of the genera in the *Rhodobacteraceae* family [5].

**Table 2.** Cellular fatty acid composition (%) of strain ASV31$^T$ and its closely phylogenetic related taxa determined under the same conditions. Strains: 1, ASV31$^T$; 2, *Thioclava pacifica* DSM 10166$^T$; 3, *Rhodovulum algae* LMG 29228$^T$. All data from this study.

| Fatty Acid | 1 | 2 | 3 |
|---|---|---|---|
| Saturated: | | | |
| $C_{16:0}$ | 5.33 | 1.71 | 16.22 |
| $C_{17:0}$ | TR | - | - |
| $C_{18:0}$ | 1.45 | 3.06 | 3.25 |
| Unsaturated: | | | |
| $C_{15:1}$ ω8c | TR | - | - |
| $C_{20:2}$ ω6,9c | 1.04 | - | - |
| Branched: | | | |
| $C_{18:1}$ ω7c 11-metilo | 8.13 | - | - |
| $C_{19:0}$ cyclo ω8c | 38.16 | - | - |
| $C_{19:0}$ 10-metilo | 3.35 | 1.12 | - |
| $C_{16:1}$ ω7c alcohol | - | - | TR |
| Hydroxy: | | | |
| $C_{10:0}$ 3OH | - | 5.14 | 3.24 |
| $C_{12:0}$ 2OH | - | 1.03 | TR |
| $C_{18:0}$ 3OH | - | 4.85 | - |
| Summed Feature 2 [1] | 2.11 | - | 1.56 |
| Summed Feature 3 [1] | TR | - | 2.97 |
| Summed Feature 7 [1] | 1.08 | - | 1.19 |
| Summed Feature 8 [1] | 37.34 | 83.08 | 70.12 |

[1] Summed features are groups of two or three fatty acids that cannot be separated by GLC with the MIDI system. Summed Feature 2 consists of C14:0 3OH and/or C16:1 iso I and/or C12:0 aldehyde. Summed Feature 3 consists of C16:1 ω7c and/or C16:1 ω6c. Summed Feature 7 consists of C18.846 and/or C19:1 ω6c and/or C19:0 cyclo ω10c. Summed Feature 8 consists of C18:1 ω7c and/or C18:1 ω6c. –, not detected; TR, trace (<1%).

### *3.3. Genome-Based Characterisation and Properties*

As shown above, the 16S rRNA-based phylogeny and phenotypic characteristics supported the hypothesis that strain ASV31$^T$ could be a new genus. However, it is argued that modern analysis approaches, such as the use of overall genome-related indexes (OGRIs) or phylogenomic tree construction, must necessarily account for effectively establishing the taxonomic position of a strain [9]. For that purpose, whole-genome sequencing of the strain was performed. Sequencing data were deposited at GenBank under accession number JAHQZS000000000. The genome size of strain ASV31$^T$ was 3.6 Mbp and it was assembled into 15 contigs with an N50 value of 0.9 Mbp. Analysis with CheckM showed that the genome completeness was 100.0% and the contamination was 0.25% (an acceptable value for this data usage). The DNA G+C content of strain ASV31$^T$ was 65.7%, which was within the common range (55–70 mol%) of the family *Rhodobacteraceae* [5]. Table 3 summarises the genomic features and principal OGRI values of strain ASV31$^T$ and its closely related taxa. ANI values relative to strain ASV31$^T$ ranged from 73.9%, with *Rhodovulum algae* LMG 29228$^T$, to 72.5% with *Tropicimonas isoalkanivorans* B51$^T$. These values were lower than the threshold values for the species boundary for ANI (95–96%) [9]. In addition, dDDH values were also below the cut-off of 70% established for species differentiation [42], with values ranging from 19.3% to 18.5% for *Haematobacter massiliensis* CCUG 47968$^T$ and *Tropicimonas isoalkanivorans* B51$^T$, respectively. These values were below the thresholds required for bacteria species description. However, Qin et al. [32] demonstrated that ANI and dDDH values were not suitable for use in genus demarcation.

**Table 3.** Genomic features of strain ASV31$^T$ and its closely related taxa, and OGRI values obtained after their genome comparison with the ASV31$^T$ genome. Data are from this study.

| Strains | Genome Size (Mbp) | DNA G+C Content (%) | ANI (%) | dDDH (%) | AAI (%) | POCP (%) |
|---|---|---|---|---|---|---|
| | | | ASV31$^T$ | ASV31$^T$ | ASV31$^T$ | ASV31$^T$ |
| *Anianabacter salinae* ASV31$^T$ | 3.6 | 65.7 | - | - | - | - |
| *Thioclava pacifica* DSM 10166$^T$ | 3.7 | 63.9 | 72.8 | 18.9 | 61.3 | 56.0 |
| *Rhodovulum algae* LMG 29228$^T$ | 4.2 | 67.4 | 73.9 | 19.2 | 63.5 | 54.0 |
| *Tropicimonas isoalkanivorans* B51$^T$ | 4.9 | 64.6 | 72.5 | 18.5 | 62.3 | 52.0 |
| *Haematobacter massiliensis* CCUG 47968$^T$ | 4.2 | 64.5 | 72.5 | 19.3 | 60.2 | 50.0 |

ANI, average nucleotide identity; dDDH, digital DNA–DNA hybridisation; AAI, average amino acid identity; POCP, percentage of conserved proteins.

In order to determine a better taxonomic position for strain ASV31$^T$ in the *Rhodobacteraceae* family, a complete AAI and POCP comparison matrix was constructed (Table S1). Strain ASV31$^T$ shared similarities of 64–66% for AAI and 54–62% for POCP with *Rhodovulum* species, 60–63% for AAI and 49–58% for POCP with *Rhodobacter* species, 60–63% for AAI and 54–58% for POCP with *Thioclava* species, 62% for AAI and 52–55% for POCP with *Tropicimonas* species and 60% for AAI and 49–50% for POCP with *Haematobacter* species. Some specific AAI boundaries have been proposed for delineation of genera in several families. In the case of *Rhodobacteraceae*, AAI values between members of related but different genera typically vary between 60–80% and do not exceed 85%. This range was used by different authors to perform genus differentiation [43,44]. In this study, the highest similarity value was observed between ASV31$^T$ and *Rhodovulum robiginosum*, with an AAI of 66.0%. These results were enough to suggest that strain ASV31$^T$ may be a new genus in the family *Rhodobacteraceae*, particularly when interspecies AAI values of genus *Rhodovulum* are more than 70% and members of the genus *Thioclava* share more than 70% AAI similarity between them, as shown in Table S1.

Our POPC results suggested that the 50% boundary for POCP is not an appropriate metric for delineating genera within the family *Rhodobacteraceae*, as *Rhodovulum* species have POCP values higher than 60% between them. The same occurs in *Thioclava* species. POCP results among the *Rhodobacter* group are more diverse, but values from 49% to 86% were found between species of that group (Table S1). The POCP limit of 50% has also not been useful for genus delimitation in the *Methylococcaceae* [45], *Bacillaceae* [46], *Burkholderiaceae* [47] and *Neisseriaceae* [48].

Furthermore, the phylogenomic tree based on whole-genome sequences showed phylogenetic separation of strain ASV31$^T$ from known clades (Figure S5). The same was observed in the RpoC-, acyl-CoA synthetase- and 2-oxoglutarate dehydrogenase-based phylogenies (Figures S6–S8). In the case of the RpoC protein, the most similar amino acid sequence was from *Tranquillimonas alkanivorans* (89.4% similarity). For acyl-CoA synthase, the most similar sequence was from *Meinhardsimonia xiamenensis* (74.4%), and in the case of 2-oxoglutarate dehydrogenase E1 component, the most similar sequence was from *Actibacterium* sp. (85.2%).

In addition to the above, an annotation of the genome was used to predict several characteristics of strain ASV31$^T$. A total of 3619 coding sequences and 48 RNAs (45 tRNAs and 3 rRNAs) was found. The subsystem category distribution showed 17.1% of genes putatively encoding amino acids and derivatives, 13.8% encoding carbohydrates, 12.9% involved in protein metabolism, and 8.4% of genes related with cofactors, vitamins, prosthetic groups and pigments. The remaining categories were found in minor percentages.

Metabolic reconstruction was performed in strain ASV31$^T$ and compared with *Thioclava pacifica* DSM 10166$^T$, *Rhodovulum algae* LMG 29228$^T$, *Tropicimonas isoalkanivorans* B51$^T$ and *Haematobacter massiliensis* CCUG 47968$^T$ (Table S2). Thirty-nine different roles, belonging to different subsystems, were found in ASV31$^T$ that were not present in any of the compared relatives. Several genes and enzymes linked with the degradation of aromatic compounds were present only in ASV31$^T$, which included the following subsystems: aro-

matic amine catabolism, benzoate degradation, the catechol branch of the beta-ketoadipate pathway and the central meta-cleavage pathway of aromatic compound degradation. Indeed, we detected genes for ring cleavage enzymes, such as catechol 1,2 dioxygenase (EC. 1.13.11.1) and protocatechuate 3,4-dioxygenase (EC. 1.13.11.3), that produce dearomatised products that are further degraded by the genes in the beta-ketoadipate pathway to central metabolites that enter the TCA cycle [49]. Studies have shown that the beta-ketoadipate pathway for the conversion of aromatic lignocellulose waste into bio-oils can be used to produce biodiesel [50] and that the central meta-cleavage pathway is described in many organisms that degrade a high quantity of phenol [51]. The presence of different genes related to the degradation of aromatic compounds in ASV31$^T$ may signify a probable role of that strain in remediation.

Other relevant subsystems only found in ASV31$^T$ were tripartite ATP-independent periplasmic (TRAP) transporters and cyanate hydrolysis. The first characterisation and naming of TRAP transporters was described in *Rhodobacter capsulatus* as the sole uptake route for malate, succinate and fumarate substrates in *R. capsulatus* grown chemoheterotrophically in the dark [52]. Subsequent studies found that TRAP transporters were widespread among bacteria and archaea from marine environments, considering it an ancient type of solute uptake system that transports a variety of substrates under different contexts [53]. Regarding cyanate hydrolysis, a putative cyanate ($NCO^-$) ABC-type transporter was only found in the ASV31$^T$ genome. Maeda and Omata (2009) [54] demonstrated that this bispecific cyanate/nitrite transporter was induced under nitrogen-deficient conditions, and its physiological role in *Synechococcus elongatus*, which is to allow nitrogen-deficient cells to assimilate low concentrations of cyanate, was also described.

In contrast, 26 different roles belonging to different subsystems were found in the relatives' genomes but not in that of ASV31$^T$. One of the most relevant differences was related to motility and chemotaxis. All essential proteins for motility, including FlgB, FlgC, FliE, FlaA, FlgH, FlhA, FlhB, FliR, MotA, FliN and FliI, were identified in the genome of the three relatives, but not in strain ASV31$^T$, which accorded with the phenotypic characterisation carried out in this study. Bartling et al. [55] concluded that 50% of the *Roseobacter* strains analysed in their study were non-motile, so this characteristic is usual in this family; in any case, it is described that *Rhodobacteraceae* members, when motile, exhibit a flagella, which is usually polar [5]. In addition to this, through genome annotation it was confirmed that strain ASV31$^T$ was not able to synthesise ribulose-1,5-bisphosphate carboxylase/oxygenase (RubisCO) small and large chain (EC 4.1.1.39), and that the RuBisCO operon transcriptional regulator CbbR was not present. The RubisCo is a key enzyme responsible for biological $CO_2$ assimilation, and it is known that species in genera of the *Rhodobacteraceae*, such as *Thioclava* spp. and *Rhodobacter* spp., contain the green form of type I RubisCo. Other genera, such as *Rhodobaca* and *Rubribacterium*, lack RubisCo, although they belong to the same family [5,37,39].

### *3.4. Biotechnological Potential of Strain ASV31$^T$ for the Production of Secondary Metabolites and Enzymes*

An in silico prediction of biosynthetic gene clusters (BGCs) using the antiSMASH 6.0.1 webserver revealed that five BGCs were involved in the secondary metabolism of strain ASV31$^T$. BGCs are a locally clustered group of two or more genes that together encode a biosynthetic pathway for the production of a secondary metabolite [35]. Strain ASV31$^T$ showed an ectoine biosynthetic gene cluster, which was 100% the same as the *Methylarcula marina* gene cluster (BGC0000860). This capacity was also seen in *Thioclava pacifica* DSM 10166$^T$ and *Rhodovulum algae* LMG 29228$^T$, but not in the other phylogenetically related type species analysed in the study. Like other compatible solutes, ectoine is a low-molecular mass compound that is highly soluble in water. In the environment, ectoine-coding biosynthetic genes (ectABC) and the ectoine hydroxylase gene (ectD) are activated to produce ectoine compounds and tolerate osmotic pressure [56]. In fact, ectoine-biosynthesis-related genes (L-2,4-diaminobutyric acid acetyltransferase (ectA), L-2,4-diaminobutyric acid transaminase

(ectB), L-ectoine synthase (ectC) and ectoine hydroxylase (ectD)) were also annotated with RAST. A number of commercial applications for ectoines have been developed to serve as water-attracting and water-structure-forming compounds, to stabilise macromolecules and entire cells through their chaperon and glass-forming effects, to protect DNA from ionising radiation and to prevent UV-induced cell damage to skin cells, among others [56].

The synthesis of a terpene biosynthetic gene cluster 100% similar to the *Rhodobacter sphaeroides* gene cluster (BGC0000647) was found in ASV31$^T$. This cluster was also observed in *Rhodovulum algae* LMG 29228$^T$, but not in the other related taxa that were compared. The terpene gene cluster is responsible for producing a wide range of functionally diverse secondary metabolites, such as carotenoids, which provide colourful pigments, including geosmin, an odorous metabolite and syctonemin that is a secondary metabolite synthesised in response to UV exposure and is produced mainly by *Cyanobacteria* [57]. Furthermore, due to the structural diversity of terpenoids, they are recognised in industrial applications as pharmaceuticals, flavourings, fragrances, antimicrobials, pesticides and alternative fuels [58].

Other BGCs found in ASV31$^T$ were a homoserine lactone cluster, an unspecified ribosomally synthesised and post-translationally modified peptide product (RiPP) cluster and a RiPP recognition element-containing cluster. These clusters had no matches with any similar known cluster. Even so, an MIBiG (minimum information about a biosynthetic gene cluster) comparison suggested a 0.16% similarity score between the homoserine lactone type cluster and the allylmalonyl-CoA compound from *Streptomyces tsukubensiscitrulas* (BGC0000886.1). The autoinducer signals from Gram-negative *Proteobacteria*, as quorum-sensing mechanisms, are generally N-acyl homoserine lactones which differ in their length and the substitution of their respective acyl side chains, conferring upon them signal specificity. However, quorum sensing has not been largely studied on halophilic organisms [59]. Nevertheless, Llamas et al. [59] discovered that all *Halomonas* strains examined in their study synthesised detectable homoserine lactones signal molecules. Furthermore, the observation of those *Halomonas* species producing growth-phase-dependent N-acyl homoserine lactones suggested that these signal molecules might regulate cellular processes, such as exopolysaccharides production, exoenzymes secretion and/or biofilm formation, in these bacteria. MIBiG also showed 0.37% and 0.17% similarity scores between the two RiPP-type-related clusters and the citrulassin E compound (BGC0001551.1) from Streptomyces glaucescens. Citrulassin is a citrulline-containing lasso peptide [60]. Lasso peptides possess a remarkable thermal and proteolytic stability and various biological activities such as antimicrobial activity, enzyme inhibition, receptor blocking, anticancer properties and HIV antagonism. Thus, they have promising potential therapeutic effects on various diseases [61].

To identify, predict and compile the CAZyme-encoded genes in strain ASV31$^T$, a dbCAN2 server was used and its capacity to degrade complex carbon sources was also assessed. Strain ASV31$^T$ had a total of 36 CAZymes families belonging to five different CAZymes categories (Table S3). A total of 14 different CAZymes families belonging to the glycosyltransferase (GT) category (enzymes responsible for the formation of glycosidic bonds), 11 families belonging to the glycoside hydrolase (GH) category (enzymes responsible for the hydrolysis of glycosidic bonds), six families in the auxiliary activities (AAs) category (redox enzymes), four families in the carbohydrate esterase (CE) category (enzymes that perform hydrolysis of carbohydrate esters) and one family in the carbohydrate-binding module (CBM) category (enzymes responsible for adhesion to carbohydrates) was found. Families belonging to the GT and GH categories were the most abundant in strain ASV31$^T$. In particular, the CAZymes acting on glycosidic bonds have proven to be crucial for significant biotechnological advances within sectors that include bioenergy and bio-based (food/feed, materials and chemicals) industries. For example, the use in biotechnology of marine-fungi-derived CAZymes has been reported due to their ability to function at a high salinity, low water potential, high sodium ion concentration and under oligotrophic nutrient conditions, among other factors [62].

The genome-guided bioprospecting of halophilic microorganisms could serve as a useful means of discovering many potential novel enzymes or bioactive molecules present in microorganisms, which may be missed when using only culture-based bioprospecting approaches. Therefore, our observations of the biosynthetic gene clusters and CAZyme-encoded genes in the genome of the novel strain ASV31$^T$ could aid the further development of ASV31$^T$ as an interesting producer of commercially high-value natural products and help improve our understanding of the ecology of halophiles.

## 4. Conclusions

The discovery of a new bacterial species is always enriching and demonstrates the immense diversity that different ecosystems possess, especially when they are places as special as ancestral salterns that are still in use. This increases knowledge, in this case, of extremophile microorganisms and their importance in such unique habitats. After analysing all the results presented in this study, we conclude that strain ASV31$^T$ is phylogenetically and phenotypically distinct from other described members of the family *Rhodobacteraceae*, i.e., members of the genera *Thioclava*, *Rhodovulum*, *Tropicimonas* and *Haematobacter*. These differences were also supported by the genomic information, which stabilised genetic differences between closest relatives. Therefore, we propose to classify this strain as representing the first species of a novel genus within the family *Rhodobacteraceae*, for which the name *Anianabacter salinae* gen. nov. sp. nov. is proposed, being the type strain ASV31$^T$ (= CECT 30309$^T$ = LMG 32242$^T$).

*Description of Anianabacter salinae gen. nov. sp. nov.*

*Anianabacter salinae* (A.nia.na.bac'ter. L. neut. adj. *Aniana*, of the Añana solar saltern; N.L. masc. n. *bacter* masc. equivalent of the Gr. neut. n. *bakterion* a rod; N.L. masc. n. *Anianabacter* a rod from Añana solar saltern; sa.li'nae N.L. gen. fem. n. *salinae*, from salterns).

The *Anianabacter* genus includes non-motile Gram-stain-negative rods that occur singly or in aggregates with a mucous polysaccharide capsule around them. They are aerobic chemoorganotrophs and highly halotolerant. Spheroidenone, spheroidene and bacteriochlorophyll a are present. The unique ubiquinone is Q-10 and the major fatty acids are C19:0 cyclo ω8c and Summed Feature 8. The major polar lipids are phosphatidylglycerol, aminolipid, an unidentified glycolipid, an unidentified phospholipid and an unidentified lipid. The genus is a member of phylum *Proteobacteria*, class *Alphaproteobacteria*, order *Rhodobacterales* and family *Rhodobacteraceae*.

Colonies of *Anianabacter salinae* are beige-to-pink coloured. The rod cells are 2.4–2.5 μm in length and 0.4–0.5 μm wide. The species grows at pH 6.5–9.5 (optimum pH 7.0–9.5) and at temperatures between 18 and 37 °C (optimum 30 °C). It has a high NaCl tolerance of 0–23% (*w*/*v*) (optimum 3–5%). PHA granules are present inside the cells. It is catalase- and oxidase-positive and urease negative. It hydrolyses aesculin and Tween 20. Nitrate reduction occurs in this species. Enzymatic activities, such as those of alkaline phosphatase, esterase (C 4), esterase lipase (C 8), leucine arylamidase, valine arylamidase and α-glucosidase, are present. However, weak activity of cysteine arylamidase, acid phosphatase and naphthol-AS-BI-phosphohydrolase, and negative activity of lipase (C 14), α-chymotrypsin, trypsin, α- and β-galactosidases, β-glucuronidase, β-glucosidase, N-acetyl-β-glucosaminidase, α-mannosidase and α-fucosidase was observed. It was found to be resistant to polymyxin B (300 IU), vancomycin (30 μg) and streptomycin (10 μg). Its genome size is 3.6 Mbp and the DNA G+C content is 65.7%.

The type strain is ASV31$^T$ (=CECT 30309$^T$ = LMG 32242$^T$) and it was isolated from brine from the Santa Engracia natural spring in Añana Salt Valley (Spain).

The GenBank/EMBL/DDBJ accession numbers for the 16S rRNA gene sequence and draft genome are MW691205 and JAHQZS000000000, respectively.

**Supplementary Materials:** The following supporting information can be downloaded at https://www.mdpi.com/article/10.3390/d14111009/s1: Figure S1: Maximum-likelihood phylogenetic tree based on 16S rRNA gene sequences showing the relationships between *Anianabacter salinae* ASV31$^T$ and other strains of *Rhodobacteraceae* family. Figure S2: Minimum evolution phylogenetic tree based on 16S rRNA gene sequences showing the relationships between *Anianabacter salinae* ASV31$^T$ and other species of *Rhodobacteraceae* family. Figure S3: *Anianabacter salinae* ASV31$^T$ growth on marine agar medium. Figure S4: Thin-layer chromatogram of polar lipids of *Anianabacter salinae* ASV31$^T$. Figure S5: Whole-genome-based taxonomic tree, showing the position of the strain ASV31$^T$ and related strains of *Rhodobacteraceae* family. Figure S6: RpoC-based maximum-likelihood tree: A, performed with the most similar amino acidic sequences; B, performed with sequences from representatives of the *Rhodobacteraceae* family. Tree was generated using MEGA X. Only bootstrap values (expressed as percentages of 1000 replications) greater than 50% are shown at branching points. The scale bar indicates the number of substitutions per site. Figure S7: Acyl-CoA synthetase-based maximum-likelihood tree: A, performed with the most similar amino acidic sequences; B, performed with sequences from representatives of the *Rhodobacteraceae* family. Tree was generated using MEGA X. Only bootstrap values (expressed as percentages of 1000 replications) greater than 50% are shown at branching points. The scale bar indicates the number of substitutions per site. Figure S8: 2-oxoglutarate dehydrogenase-based maximum likelihood tree; A, performed with the most similar amino acidic sequences, B, performed with sequences from representatives of the *Rhodobacteraceae* family. Tree was generated using MEGA X. Only bootstrap values (expressed as percentages of 1000 replications) greater than 50% are shown at branching points. The scale bar indicates the number of substitutions per site. Table S1: AAI and POCP matrix from pairwise whole-genome comparison. Table S2: Presence and absence of subsystems in strain ASV31$^T$ compared to its closest relatives. Table S3: CAZyme types present in ASV31$^T$ strain.

**Author Contributions:** Conceptualisation, I.M.-B., J.G. and J.B.; methodology, I.M.-B. and J.G.; formal analysis, M.A.-M., M.G., L.L., I.M.-M., S.S. and I.M.-B.; resources, J.B.; data curation, M.A.-M., M.G., L.L., I.M.-M., S.S. and I.M.-B.; writing—original draft preparation, M.A.-M. and I.M.-B.; writing—review and editing, all authors; funding acquisition, J.G. and I.M.-B. All authors have read and agreed to the published version of the manuscript.

**Funding:** This research was funded by the University of the Basque Country UPV/EHU (grant number US19/01) and the Añana Salt Valley Foundation (specific agreement between the Añana Salt Valley Foundation and the University of the Basque Country UPV/EHU).

**Institutional Review Board Statement:** Not applicable.

**Acknowledgments:** The authors are grateful for the technical and human support provided by the UPV/EHU Advanced Research Facilities (SGIker).

**Conflicts of Interest:** The authors declare no conflict of interest.

## References

1. Landa, M.; Montero, A. *Salt Valley of Añana. Towarsds Its Full Recovery. Vallée Salée de Añana. Vers Une Récupération Intégrale*; Diputación Foral de Álava: Vitoria-Gasteiz, Spain, 2007; ISBN 978-84-7824-680-2.
2. Garrity, G.M.; Bell, J.A.; Lilburn, T. Family I. *Rhodobacteraceae* fam. nov. *Bergey's Man. Syst. Bacteriol.* **2005**, *2*, 161.
3. Hördt, A.; López, M.G.; Meier-Kolthoff, J.P.; Schleuning, M.; Weinhold, L.-M.; Tindall, B.J.; Gronow, S.; Kyrpides, N.C.; Woyke, T.; Göker, M. Analysis of 1,000+ Type-Strain Genomes Substantially Improves Taxonomic Classification of *Alphaproteobacteria*. *Front. Microbiol.* **2020**, *11*, 468. [CrossRef] [PubMed]
4. Szuróczki, S.; Abbaszade, G.; Buni, D.; Bóka, K.; Schumann, P.; Neumann-Schaal, M.; Vajna, B.; Tóth, E. *Fertoeibacter niger* gen. nov., sp. nov. a Novel Alkaliphilic Bacterium of the Family *Rhodobacteraceae*. *Int. J. Syst. Evol. Microbiol.* **2021**, *71*, 004762. [CrossRef] [PubMed]
5. Pujalte, M.J.; Lucena, T.; Ruvira, M.A.; Arahal, D.R.; Macián, M.C. The Family *Rhodobacteraceae*. In *The Prokaryotes*; Springer: Berlin/Heidelberg, Germany, 2014; pp. 439–512.
6. Liang, K.Y.; Orata, F.D.; Boucher, Y.F.; Case, R.J. Roseobacters in a Sea of Poly-and Paraphyly: Whole Genome-Based Taxonomy of the Family *Rhodobacteraceae* and the Proposal for the Split of the "*Roseobacter* Clade" into a Novel Family, *Roseobacteraceae* Fam. Nov. *Front. Microbiol.* **2021**, *12*, 1635. [CrossRef]

7. Barnier, C.; Clerissi, C.; Lami, R.; Intertaglia, L.; Lebaron, P.; Grimaud, R.; Urios, L. Description of *Palleronia Rufa* sp. nov., a Biofilm-Forming and AHL-Producing *Rhodobacteraceae*, Reclassification of *Hwanghaeicola Aestuarii* as *Palleronia Aestuarii* comb. nov., *Maribius Pontilimi* as *Palleronia Pontilimi* comb. nov., *Maribius Salinus* as *Palleronia Salina* comb. nov., *Maribius Pelagius* as *Palleronia Pelagia* comb. nov. and Emended Description of the Genus *Palleronia*. *Syst. Appl. Microbiol.* **2020**, *43*, 126018. [CrossRef]
8. Pohlner, M.; Dlugosch, L.; Wemheuer, B.; Mills, H.; Engelen, B.; Reese, B.K. The Majority of Active *Rhodobacteraceae* in Marine Sediments Belong to Uncultured Genera: A Molecular Approach to Link Their Distribution to Environmental Conditions. *Front. Microbiol.* **2019**, *10*, 659. [CrossRef]
9. Barcelos, M.C.; Vespermann, K.A.; Pelissari, F.M.; Molina, G. Current Status of Biotechnological Production and Applications of Microbial Exopolysaccharides. *Crit. Rev. Food Sci. Nutr.* **2020**, *60*, 1475–1495. [CrossRef]
10. Yin, J.; Chen, J.-C.; Wu, Q.; Chen, G.-Q. Halophiles, Coming Stars for Industrial Biotechnology. *Biotechnol. Adv.* **2015**, *33*, 1433–1442. [CrossRef]
11. Park, S.; Lee, B.; Park, K. Extremophilic Carbohydrate Active Enzymes (CAZymes). *J. Nutr. Health Food Eng.* **2017**, *7*, 230–237. [CrossRef]
12. Weisburg, W.G.; Barns, S.M.; Pelletier, D.A.; Lane, D.J. 16S Ribosomal DNA Amplification for Phylogenetic Study. *J. Bacteriol.* **1991**, *173*, 697–703. [CrossRef]
13. Yoon, S.-H.; Ha, S.-M.; Kwon, S.; Lim, J.; Kim, Y.; Seo, H.; Chun, J. Introducing EzBioCloud: A Taxonomically United Database of 16S RRNA Gene Sequences and Whole-Genome Assemblies. *Int. J. Syst. Evol. Microbiol.* **2017**, *67*, 1613. [CrossRef] [PubMed]
14. Kumar, S.; Stecher, G.; Li, M.; Knyaz, C.; Tamura, K. MEGA X: Molecular Evolutionary Genetics Analysis across Computing Platforms. *Mol. Biol. Evol.* **2018**, *35*, 1547. [CrossRef] [PubMed]
15. Saitou, N.; Nei, M. The Neighbor-Joining Method: A New Method for Reconstructing Phylogenetic Trees. *Mol. Biol. Evol.* **1987**, *4*, 406–425. [CrossRef] [PubMed]
16. Fitch, W.M.; Margoliash, E. Construction of Phylogenetic Trees. *Science* **1967**, *155*, 279–284. [CrossRef]
17. Felsenstein, J. Confidence Limits on Phylogenies: An Approach Using the Bootstrap. *Evolution* **1985**, *39*, 783–791. [CrossRef]
18. Smith, A.C.; Hussey, M.A. Gram Stain Protocols. *Am. Soc. Microbiol.* **2005**, *1*, 14.
19. Zapata, M.; Rodríguez, F.; Garrido, J.L. Separation of Chlorophylls and Carotenoids from Marine Phytoplankton: A New HPLC Method Using a Reversed Phase C8 Column and Pyridine-Containing Mobile Phases. *Mar. Ecol. Prog. Ser.* **2000**, *195*, 29–45. [CrossRef]
20. Seoane, S.; Zapata, M.; Orive, E. Growth Rates and Pigment Patterns of Haptophytes Isolated from Estuarine Waters. *J. Sea Res.* **2009**, *62*, 286–294. [CrossRef]
21. Mesquita, D.P.; Amaral, A.L.; Leal, C.; Oehmen, A.; Reis, M.A.M.; Ferreira, E.C. Polyhydroxyalkanoate Granules Quantification in Mixed Microbial Cultures Using Image Analysis: Sudan Black B versus Nile Blue A Staining. *Anal. Chim. Acta* **2015**, *865*, 8–15. [CrossRef]
22. Santhanam, A.; Sasidharan, S. Microbial Production of Polyhydroxy Alkanotes (PHA) from *Alcaligens* spp. and *Pseudomonas oleovorans* Using Different Carbon Sources. *Afr. J. Biotechnol.* **2010**, *9*, 3144–3150.
23. Sasser, M. *Identification of Bacteria by Gas Chromatography of Cellular Fatty Acids*; MIDI Technical Note 101; MIDI Inc.: Newark, DE, USA, 1990.
24. MIDI. *Sherlock Microbial Identification System Operating Manual*; Version 6.1; MIDI Inc.: Newark, DE, USA, 2008.
25. Bligh, E.G.; Dyer, W.J. A rapid method of total lipid extraction and purification. *Can. J. Biochem. Physiol.* **1959**, *37*, 911–917. [CrossRef] [PubMed]
26. Tindall, B.J.; Sikorski, J.; Smibert, R.M.; Kreig, N.R. Phenotipic characterization and the principlen of comparative systematics. In *Methods for General and MOlecular Microbiology*, 3rd ed.; Reddy, C.A., Beveridge, T.J., Breznak, J.A., Marluf, G.A., Schmidt, T.M., Snyder, L.R., Eds.; ASM Press: Washington, DC, USA, 2007; pp. 330–393.
27. Davis, J.J.; Wattam, A.R.; Aziz, R.K.; Brettin, T.; Butler, R.; Butler, R.M.; Chlenski, P.; Conrad, N.; Dickerman, A.; Dietrich, E.M. The PATRIC Bioinformatics Resource Center: Expanding Data and Analysis Capabilities. *Nucleic Acids Res.* **2020**, *48*, D606–D612. [CrossRef] [PubMed]
28. Parks, D.H.; Imelfort, M.; Skennerton, C.T.; Hugenholtz, P.; Tyson, G.W. CheckM: Assessing the Quality of Microbial Genomes Recovered from Isolates, Single Cells, and Metagenomes. *Genome Res.* **2015**, *25*, 1043–1055. [CrossRef] [PubMed]
29. Yoon, S.-H.; Ha, S.; Lim, J.; Kwon, S.; Chun, J. A Large-Scale Evaluation of Algorithms to Calculate Average Nucleotide Identity. *Antonie Van Leeuwenhoek* **2017**, *110*, 1281–1286. [CrossRef] [PubMed]
30. Meier-Kolthoff, J.P.; Göker, M. TYGS Is an Automated High-Throughput Platform for State-of-the-Art Genome-Based Taxonomy. *Nat. Commun.* **2019**, *10*, 2182. [CrossRef] [PubMed]
31. Rodriguez-R, L.M.; Konstantinidis, K.T. Bypassing Cultivation to Identify Bacterial Species. *Microbe Mag.* **2014**, *9*, 111–118. [CrossRef]
32. Qin, Q.-L.; Xie, B.-B.; Zhang, X.-Y.; Chen, X.-L.; Zhou, B.-C.; Zhou, J.; Oren, A.; Zhang, Y.-Z. A Proposed Genus Boundary for the Prokaryotes Based on Genomic Insights. *J. Bacteriol.* **2014**, *196*, 2210–2215. [CrossRef]
33. Lefort, V.; Desper, R.; Gascuel, O. FastME 2.0: A Comprehensive, Accurate, and Fast Distance-Based Phylogeny Inference Program. *Mol. Biol. Evol.* **2015**, *32*, 2798–2800. [CrossRef]
34. Aziz, R.K.; Bartels, D.; Best, A.A.; DeJongh, M.; Disz, T.; Edwards, R.A.; Formsma, K.; Gerdes, S.; Glass, E.M.; Kubal, M. The RAST Server: Rapid Annotations Using Subsystems Technology. *BMC Genom.* **2008**, *9*, 75. [CrossRef]

35. Blin, K.; Shaw, S.; Kloosterman, A.M.; Charlop-Powers, Z.; Van Wezel, G.P.; Medema, M.H.; Weber, T. AntiSMASH 6.0: Improving Cluster Detection and Comparison Capabilities. *Nucleic Acids Res.* **2021**, *49*, W29–W35. [CrossRef]
36. Zhang, H.; Yohe, T.; Huang, L.; Entwistle, S.; Wu, P.; Yang, Z.; Busk, P.K.; Xu, Y.; Yin, Y. DbCAN2: A Meta Server for Automated Carbohydrate-Active Enzyme Annotation. *Nucleic Acids Res.* **2018**, *46*, W95–W101. [CrossRef] [PubMed]
37. Zhang, R.; Lai, Q.; Wang, W.; Li, S.; Shao, Z. *Thioclava dalianensis* sp. nov., Isolated from Surface Seawater. *Int. J. Syst. Evol. Microbiol.* **2013**, *63*, 2981–2985. [CrossRef] [PubMed]
38. Ramaprasad, E.V.V.; Tushar, L.; Dave, B.; Sasikala, C.; Ramana, C.V. *Rhodovulum algae* sp. nov., Isolated from an Algal Mat. *Int. J. Syst. Evol. Microbiol.* **2016**, *66*, 3367–3371. [CrossRef]
39. Sorokin, D.Y.; Tourova, T.P.; Spiridonova, E.M.; Rainey, F.A.; Muyzer, G. *Thioclava pacifica* gen. nov., sp. nov., a Novel Facultatively Autotrophic, Marine, Sulfur-Oxidizing Bacterium from a near-Shore Sulfidic Hydrothermal Area. *Int. J. Syst. Evol. Microbiol.* **2005**, *55*, 1069–1075. [CrossRef]
40. Harwati, T.U.; Kasai, Y.; Kodama, Y.; Susilaningsih, D.; Watanabe, K. *Tropicimonas isoalkanivorans* gen. nov., sp. nov., a Branched-Alkane-Degrading Bacterium Isolated from Semarang Port in Indonesia. *Int. J. Syst. Evol. Microbiol.* **2009**, *59*, 388–391. [CrossRef]
41. Helsel, L.O.; Hollis, D.; Steigerwalt, A.G.; Morey, R.E.; Jordan, J.; Aye, T.; Radosevic, J.; Jannat-Khah, D.; Thiry, D.; Lonsway, D.R. Identification of "*Haematobacter*," a New Genus of Aerobic Gram-Negative Rods Isolated from Clinical Specimens, and Reclassification of *Rhodobacter massiliensis* as "*Haematobacter massiliensis* comb. *nov.*" *J. Clin. Microbiol.* **2007**, *45*, 1238–1243. [CrossRef] [PubMed]
42. Chun, J.; Oren, A.; Ventosa, A.; Christensen, H.; Arahal, D.R.; da Costa, M.S.; Rooney, A.P.; Yi, H.; Xu, X.-W.; De Meyer, S. Proposed Minimal Standards for the Use of Genome Data for the Taxonomy of Prokaryotes. *Int. J. Syst. Evol. Microbiol.* **2018**, *68*, 461–466. [CrossRef]
43. Wirth, J.S.; Whitman, W.B. Phylogenomic Analyses of a Clade within the *Roseobacter* Group Suggest Taxonomic Reassignments of Species of the Genera *Aestuariivita*, *Citreicella*, *Loktanella*, *Nautella*, *Pelagibaca*, *Ruegeria*, *Thalassobius*, *Thiobacimonas* and *Tropicibacter*, and the Proposal of Six Novel Genera. *Int. J. Syst. Evol. Microbiol.* **2018**, *68*, 2393–2411. [CrossRef]
44. Suresh, G.; Lodha, T.D.; Indu, B.; Sasikala, C.; Ramana, C.V. Taxogenomics Resolves Conflict in the Genus *Rhodobacter*: A Two and Half Decades Pending Thought to Reclassify the Genus *Rhodobacter*. *Front. Microbiol.* **2019**, *10*, 2480. [CrossRef]
45. Orata, F.D.; Meier-Kolthoff, J.P.; Sauvageau, D.; Stein, L.Y. Phylogenomic Analysis of the Gammaproteobacterial Methanotrophs (Order *Methylococcales*) Calls for the Reclassification of Members at the Genus and Species Levels. *Front. Microbiol.* **2018**, *9*, 3162. [CrossRef]
46. Aliyu, H.; Lebre, P.; Blom, J.; Cowan, D.; De Maayer, P. Phylogenomic Re-Assessment of the Thermophilic Genus *Geobacillus*. *Syst. Appl. Microbiol.* **2016**, *39*, 527–533. [CrossRef] [PubMed]
47. Lopes-Santos, L.; Castro, D.B.A.; Ferreira-Tonin, M.; Corrêa, D.B.A.; Weir, B.S.; Park, D.; Ottoboni, L.M.M.; Neto, J.R.; Destéfano, S.A.L. Reassessment of the Taxonomic Position of *Burkholderia andropogonis* and Description of *Robbsia andropogonis* gen. nov., comb. nov. *Antonie Van Leeuwenhoek* **2017**, *110*, 727–736. [CrossRef] [PubMed]
48. Li, Y.; Xue, H.; Sang, S.; Lin, C.; Wang, X. Phylogenetic Analysis of Family *Neisseriaceae* Based on Genome Sequences and Description of *Populibacter corticis* gen. nov., sp. nov., a Member of the Family *Neisseriaceae*, Isolated from Symptomatic Bark of *Populus* x *euramericana* Canker. *PLoS ONE* **2017**, *12*, e0174506. [CrossRef] [PubMed]
49. Marsh, W.S.; Heise, B.W.; Krzmarzick, M.J.; Murdoch, R.W.; Fathepure, B.Z. Isolation and Characterization of a *Halophilic modicisalibacter* sp. Strain Wilcox from Produced Water. *Sci. Rep.* **2021**, *11*, 6943. [CrossRef] [PubMed]
50. Wells, T., Jr.; Ragauskas, A.J. Biotechnological Opportunities with the β-Ketoadipate Pathway. *Trends Biotechnol.* **2012**, *30*, 627–637. [CrossRef]
51. Mahiudddin, M.; Fakhruddin, A.N.M. Degradation of Phenol via Meta Cleavage Pathway by *Pseudomonas fluorescens* PU1. *ISRN Microbiol.* **2012**, *2012*, 1–6. [CrossRef]
52. Forward, J.A.; Behrendt, M.C.; Wyborn, N.R.; Cross, R.; Kelly, D.J. TRAP Transporters: A New Family of Periplasmic Solute Transport Systems Encoded by the DctPQM Genes of *Rhodobacter capsulatus* and by Homologs in Diverse Gram-Negative Bacteria. *J. Bacteriol.* **1997**, *179*, 5482–5493. [CrossRef]
53. Rosa, L.T.; Bianconi, M.E.; Thomas, G.H.; Kelly, D.J. Tripartite ATP-Independent Periplasmic (TRAP) Transporters and Tripartite Tricarboxylate Transporters (TTT): From Uptake to Pathogenicity. *Front. Cell. Infect. Microbiol.* **2018**, *8*, 33. [CrossRef]
54. Maeda, S.; Omata, T. Nitrite Transport Activity of the ABC-Type Cyanate Transporter of the Cyanobacterium *Synechococcus elongatus*. *J. Bacteriol.* **2009**, *191*, 3265–3272. [CrossRef]
55. Bartling, P.; Vollmers, J.; Petersen, J. The First World Swimming Championships of *Roseobacters*—Phylogenomic Insights into an Exceptional Motility Phenotype. *Syst. Appl. Microbiol.* **2018**, *41*, 544–554. [CrossRef]
56. Czech, L.; Hermann, L.; Stöveken, N.; Richter, A.A.; Höppner, A.; Smits, S.H.J.; Heider, J.; Bremer, E. Role of the Extremolytes Ectoine and Hydroxyectoine as Stress Protectants and Nutrients: Genetics, Phylogenomics, Biochemistry, and Structural Analysis. *Genes* **2018**, *9*, 177. [CrossRef] [PubMed]
57. Chen, R.; Wong, H.L.; Kindler, G.S.; MacLeod, F.I.; Benaud, N.; Ferrari, B.C.; Burns, B.P. Discovery of an Abundance of Biosynthetic Gene Clusters in Shark Bay Microbial Mats. *Front. Microbiol.* **2020**, *11*, 1950. [CrossRef] [PubMed]
58. Reddy, G.K.; Leferink, N.G.H.; Umemura, M.; Ahmed, S.T.; Breitling, R.; Scrutton, N.S.; Takano, E. Exploring Novel Bacterial Terpene Synthases. *PLoS ONE* **2020**, *15*, e0232220. [CrossRef] [PubMed]

59. Llamas, I.; Quesada, E.; Martínez-Cánovas, M.J.; Gronquist, M.; Eberhard, A.; Gonzalez, J.E. Quorum Sensing in Halophilic Bacteria: Detection of N-Acyl-Homoserine Lactones in the Exopolysaccharide-Producing Species of Halomonas. *Extremophiles* **2005**, *9*, 333–341. [CrossRef]
60. Harris, L.A.; Saint-Vincent, P.M.B.; Guo, X.; Hudson, G.A.; DiCaprio, A.J.; Zhu, L.; Mitchell, D.A. Reactivity-Based Screening for Citrulline-Containing Natural Products Reveals a Family of Bacterial Peptidyl Arginine Deiminases. *ACS Chem. Biol.* **2020**, *15*, 3167–3175. [CrossRef] [PubMed]
61. Cheng, C.; Hua, Z.-C. Lasso Peptides: Heterologous Production and Potential Medical Application. *Front. Bioeng. Biotechnol.* **2020**, *8*, 571165. [CrossRef]
62. Klaus, T.; Ninck, S.; Albersmeier, A.; Busche, T.; Wibberg, D.; Jiang, J.; Elcheninov, A.G.; Zayulina, K.S.; Kaschani, F.; Bräsen, C.; et al. Activity-Based Protein Profiling for the Identification of Novel Carbohydrate-Active Enzymes Involved in Xylan Degradation in the Hyperthermophilic Euryarchaeon *Thermococcus* sp. Strain 2319x1E. *Front. Microbiol.* **2022**, *12*, 3868. [CrossRef]